5-2017

Formation of LiFePO4-Pan Submicron Fibers Via Forcespinning ® for Battery Cathode Applications

Ashlee L. Lopez
The University of Texas Rio Grande Valley

FORMATION OF $LiFePO_4$-PAN SUBMICRON FIBERS VIA FORCESPINNING® FOR BATTERY CATHODE APPLICATIONS

A Thesis

by

ASHLEE L. LOPEZ

Submitted to the Graduate College of
The University of Texas Rio Grande Valley
In partial fulfillment of the requirements for the degree of

MASTER OF SCIENCE

May 2017

Major Subject: Chemistry

FORMATION OF $LiFePO_4$-PAN SUB-MICRON FIBERS VIA FORCESPINNING® FOR BATTERY CATHODE APPLICATIONS

A Thesis
by
ASHLEE L. LOPEZ

COMMITTEE MEMBERS

Dr. Tulay Atesin
Chair of Committee

Dr. Mataz Alcoutlabi
Committee Member

Dr. Javier Macossay-Torres
Committee Member

May 2017

ABSTRACT

Lopez, Ashlee L., Formation of $LiFePO_4$/PAN Submicron-fibers via Forcespinning® for Battery Cathode Applications. Master of Science (MS), May, 2017, 23 pp., 3 tables, 16 figures, references, 14 titles.

LiFePO4/C composite nanofibers were prepared by utilizing Forcespinning® technology and calcination approaches. Polyacrylonitrile (PAN) was dissolved in N, N-dimethylformamide (DMF) to produce the media that allotted fiber formation via Forcespinning®. A LiFePO4 solution was synthesized separately in DMF, which served as the precursor for the cathode material. The separately prepared PAN/DMF and LiFePO4/DMF solutions were then mixed at different weight percent's (wt.%) prior to being subjected to Forcespinning®. Elemental analysis of the LiFePO4/PAN nanofibers was characterized by energy dispersive spectroscopy (EDS) and x-ray photoelectron spectroscopy (XPS). The study of the surface morphology was conducted by scanning electron microscopy (SEM). Structural analysis of the LiFePO4/C composite nanofibers was studied utilizing x-ray diffraction (XRD) and Raman analysis. Lastly, the electrochemical analysis of the LiFePO4/C composite nanofibers was studied in coin type cells. As a result a methodology was standardized to successfully produce LiFePO4/C composite submicron-nanofibers via Forcespinning®.

TABLE OF CONTENTS

Page

LIST OF TABLES

Page

LIST OF FIGURES

Page

CHAPTER I

INTRODUCTION

Due to limited resources and over utilization of energy consumption, there is a strong necessity for innovative and efficient energy storage materials. Electricity production is highly dependent on coal and the trade offs are dismal. Renewable energy sources such as hydroelectric, wind power, and solar power techniques are up and coming however, have not yet been successfully implemented to the extent that coal has. Next generation lithium-ion batteries (LIB), serve as a promising energy storage source that could counteract the high energy needs necessary for daily use [1]. Rechargeable lithium-ion batteries are the most commonly utilized energy storage systems at this time. They are used in almost every electronic device out on the market and have intended future applications for electronic vehicles [1]. These rechargeable LIB are sought after due to offering greater energy and power densities, take less space, and deliver more energy compared to Ni-MH, Ni-Cd, and Pb acid batteries [2]. Other advantages of rechargeable LIB are attributed to the long cycle life, low self-discharge, high operating voltage, wide temperature window, and no memory effect [1].

The mechanism pertaining to the charge and discharging of the rechargeable LIB is illustrated in Figure 1. Every LIB contains a cathode ($LiFePO_4$) and an anode (carbon source) that is separated by an electrolyte intercalating material denoted as the separator. When the Li deintercalates from the cathode and intercalates into the anode the battery is in the process of

charging. During the reverse process, when the Li intercalates back into the cathode passing through the electrolyte-filled separator, the battery is in the process of discharging. The flow of Li ions between the cathode and anode during the charge/discharging process enable the conversion of chemical energy into electrical energy. This ultimately is the mechanism responsible for the storage of electrochemical energy within the battery [1].

The success of the LIB corresponds to the starting materials utilized for Li storage in the batteries. The cathode is mainly prepared from material that contains characteristically high positive redox potentials such as $LiCoO_2$, $LiMn_2O_4$, and pertaining to this study, $LiFePO_4$. In regards to the anode, graphite is the most utilized material for LIB due to the low and flat working potential, long cycle life, and low cost [1]. Past work has utilized electrospun nanofibers for LIB rather than active powder materials used today. Composite nanofibers are found to contain short-diffusion distances and high-lithium diffusion coefficients that are attributed to their one-dimensional structure. Due to these characteristics, nanofibers experience large capacity, high charge/discharge rate attributes, and extended life cycle [2].

Nanofiber formation for LIB has for the most part been conducted solely via electrospinning and studied mainly by Toprakci and Alcoutlabi. This technique utilizes a high electric field and driving a polymer solution through it producing nanofibers. A high voltage is necessary to form a liquid jet composed of a solution with low viscosity. This liquid jet is continuously stretched due to electrostatic repulsions between the charges on the surface and the solvent evaporating [3]. This approach consists of three major units: a high-voltage power supply, a spinneret, and a grounded conductor to collect the fibers. For electrospinning a high voltage within the range of 1-30 kV is applied to the polymer solution and becomes greatly electrified throughout the surface. The polymer solution then experiences electrostatic

repulsions and a Coulombic force that is exerted by the outer electric field. The fiber is ultimately formed via the whipping and stretching along the electric field [3]. Electrospinning has a nanofiber production yield of approximately 0.1g/h and requires high current and voltage specifications, which brings up safety concerns that ultimately prevents this technique to successfully mass-produce fibers [4]. Although electrospinning has been studied extensively regarding the formation of nanofibers, it is not the only technique utilized today. The set backs pertaining to electrospinning are addressed with the novel method of Forcespinning developed by Sarkar, Lozano et al [4].

Forcespinning technology replaces the electric field analogous to the electrospinning method with centrifugal forces. The setup for this system consists of a spinneret, a control system, motor, and a brake. This along with multi configurations of interchangeable spinnerets warrants Forscespinning® as an adaptable technique that overcomes the limitations pertaining to electrospinning such as, having a high electric field and employing solutions that are dielectric. This method does not require conductive solutions therefore nanofibers can be spun from a wide range of materials that may or may not be conductive [5]. Since Forcespinning® does not require a high voltage environment to produce nanofibers, this makes it a practical and safer technique to implement for nanofiber production.

CHAPTER II

EXPERIMENTAL METHODS AND MATERIALS

2.1 Materials

The starting materials for the preparation of the $LiFePO_4$/PAN nanofibers, polyacrylonitrile (PAN, MW=150,000 g/mol), iron(II) sulfate heptahydrate ($FeSO_4 \bullet 7H_2O$, $\geq$ 99.0%), and phosphoric acid (H_3PO_4, $\geq$ 85 wt. % in H_2O) were purchased from Sigma-Aldrich (Milwaukee, WI, USA) and utilized as received. Lithium acetate dihydrate ($CH_3COOLi \bullet 2H_2O$, 98%) was purchased from Arcos Organics and utilized as received. *N*,*N*-dimethylformamide (DMF) was purchased from Fischer Scientific (Waltham, MA, USA) and utilized as received. All of the starting materials were weighed on a Sartorius scale. The $LiFePO_4$ and PAN solutions were prepared separately in 20 mL Chemglass reaction vials, placed on an Opti Mag + stirring plate with a magnetic stirring bar within the solution, and allotted 24 hours (h) to stir. The separately prepared $LiFePO_4$ and PAN solutions were then mixed at different wt. % and Forcespun® to produce $LiFePO_4$/PAN nanofibers.

2.2 Synthesis of $LiFePO_4$ Solution as the Precursor

As a cathode material $LiFePO_4$ has been reported in the literature [10-14]. As an alternative route to the literature procedure, $FeSO_4 \bullet 7H_2O$, an air and moisture stable precursor was chosen as the iron source. To prepare different wt. % of $LiFePO_4$ solutions, an excel spreadsheet was utilized to aid in determining the amounts of $FeSO_4 \bullet 7H_2O$, H_3PO_4,

$CH_3COOLi•2H_2O$, and DMF that would be required. Table 2.1 and Table 2.2 show an example of how this chart was utilized. In the preparation a 14.9 wt. % solution of $LiFePO_4$ a 1:1:1 molar ratio of $CH_3COOLi•2H_2O$, H_3PO_4, $FeSO_4•7H_2O$ is obtained. Then the corresponding amounts of $CH_3COOLi•2H_2O$ was weighed and dissolved in 13.63 g of DMF, which was previously weighed out in a 20 mL glass vial and allowed to stir until completely dissolved, which required approximately 1h of stirring. Then 1.023 g of H_3PO_4 was added to the already stirring mixture and was kept continuously stirring for approximately 1 h. Lastly 2.467 g of $FeSO_4•7H_2O$ was added to the already stirring mixture and stirred for 12 h. Upon the addition of the $FeSO_4•7H_2O$, a color change was observed in the solution from an opaque-white color to a gradually darkening gray-green color. Different wt. % of $LiFePO_4$ solutions were prepared utilizing the same protocol corresponding to 1.8, 2.0, 2.4, and 14.9 wt. % respectively.

	LiOAc.2H2O	**H3PO4 (85%)**	**FeSO4.7H20**	-->	**LiFePO4**	**H2O**
MW (g/mol)	102.02	98	278.01		157.76	18
mass (g)	**0.905**	1.023	**2.467**		**1.4**	1.59
Volume (mL)		**0.607**				
mol	0.009	0.009	0.009		0.01	0.08
eq	1	1	1		1	9

Table 1. Excel Spreadsheet Utilized to Get Quantities of Starting Materials

Solution	**LiFePO4**	**PAN**	**DMF**	**H2O (from reaction)**	**Total Mass**
%	**7**	**10**	75.04	7.96	100
g (20 g)	**1.4**	**2**	15.01	1.59	**20**

Table 2. Excel Spreadsheet Utilized to Obtain Different Samples

2.3 Preparation of PAN/DMF Solution as the Medium for Fiber Formation

The polymer PAN was designated as the spinning medium due to the extensive research that has previously been conducted with electrospinning and Forcespinning®. Different wt. % of PAN/DMF solutions was prepared and it was concluded that a 20 g solution of 1 wt. % PAN in DMF, was the optimal ratio to proceed with the entirety of the experiment. The corresponding amount of PAN was dissolved in DMF and stirred for 12 h.

2.4 Combining the Separately Prepared $LiFePO_4$ and PAN Solutions

The final step prior to Forcespinning® was to combine the $LiFePO_4$/DMF and PAN/DMF solutions prepared separately. Different quantities of each solution were combined and mixed on a micro scale setup consisting of a final weight ranging from 3-4.5g as described in Table 2.3. These freshly prepared samples consisting of different amounts of $LiFePO_4$/DMF and PAN/DMF solutions were stirred in 20 mL vials over a stirring plate for approximately 12 h.

Serial #	wt% LiFePO4	wt% PAN	wt% H2o	%DMF	Total %
al-2.4p	0.9%	7.7%	1.0%	90.5%	100.1%
al-122	1.8%	10.0%	2.0%	86.3%	100.0%
160201	2.0%	10.2%	2.3%	85.5%	100.0%
al-41216	4.6%	7.4%	5.2%	82.8%	100.0%
al5	5.0%	7.1%	5.6%	82.3%	100.0%
al6	6.4%	6.1%	7.3%	80.2%	100.0%
al-41216	4.5%	9.9%	4.9%	80.7%	100.0%

Table 3. Different Wt.% of Each Sample

2.5 Formation of $LiFePO_4$/PAN Nanofibers via Forcespinning®

The solutions prepared as described in Table 2.3**,** were spun utilizing a Fiberlab L1000 Forcespinning® machine. The solutions were injected into the spinneret via a 2 mL syringe then 30 gauge (G) needles were screwed into the orifices of the spinneret. The program parameters were set for the spinneret to spin at 7000 rotations per minute (7K rpm) for 2 minutes (min).

Figure 2.1 shows the inside of the Fiberlab L 1000 machine and how the fibers appear after Forcespinning® prior to collection with a microscope slide.

Figure 1: Inside of Forcespinning® Instrument

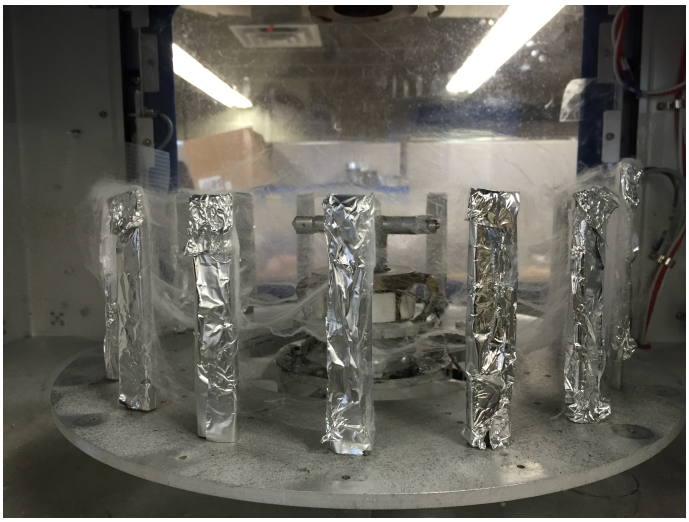

Figure 2: Collected Nanofibers After Forcespinning®

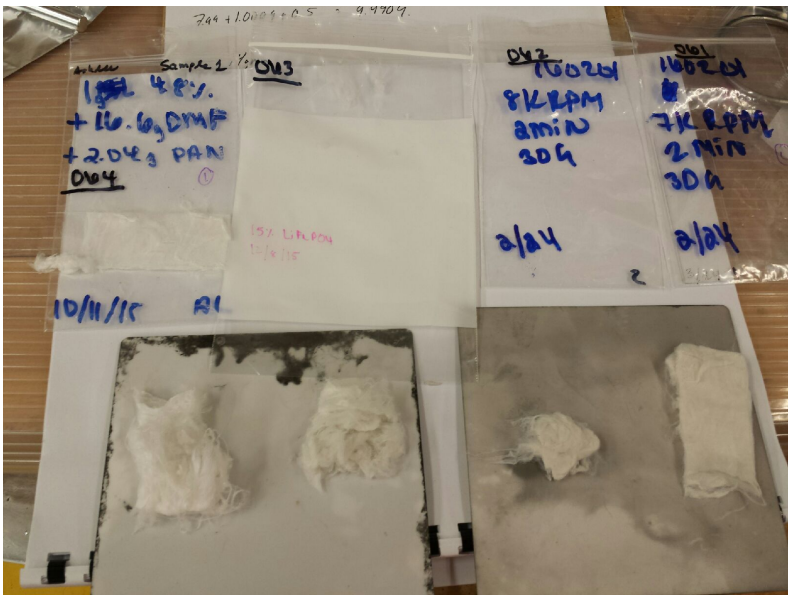

Figure 3: Collected Fibers After Forcespinning® Utilizing a Microscope Slide

2.6 Formation of $LiFePO_4$/C Composite Cathode Material via Carbonization

The fiber mat produced from samples Al5 and Al6 were collected as shown in Figure 3 and carbonized via a glass tube furnace. The samples were stabilized in air at 280 ^{o}C for 6 hours at a heating ramping rate of 5 ^{o}C / min. The samples were then carbonized in Ar at 600 ^{o}C for 8 hours at a heating ramping rate of 2 ^{o}C / min. This process is responsible for producing the $LiFePO_4$/C composite material, which will be utilized as the cathode.

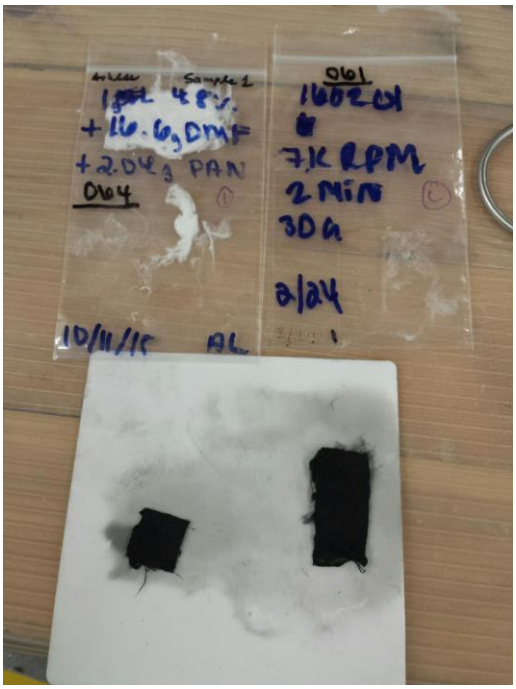

Figure 4: Carbonized Fibers

2.7 Preparation of the Coin Type Battery Cell

After carbonization, the samples were left in a vacuum oven for approximately 1 hour at 60 ^{o}C and -30 psi. The process was then moved to a glove box that was purged with Ar roughly four times. The battery cell is prepared as follows: a metal casing of the coin cell is placed at the bottom, the $LiFePO_4$/C sample is cut out and placed on top. Then a stainless steel spacer, followed by a glass separator, and another stainless steel spacer are layered on top. Ten drops of a commercial electrolyte solution is then added, followed by a spring, and then the second metal casing is placed on top. Figure 5 shows the cell with the spring on top. The battery cell is then pressed via a hydraulic press and the coin-type battery cell is completed. The cells were tested via electrochemical analysis.

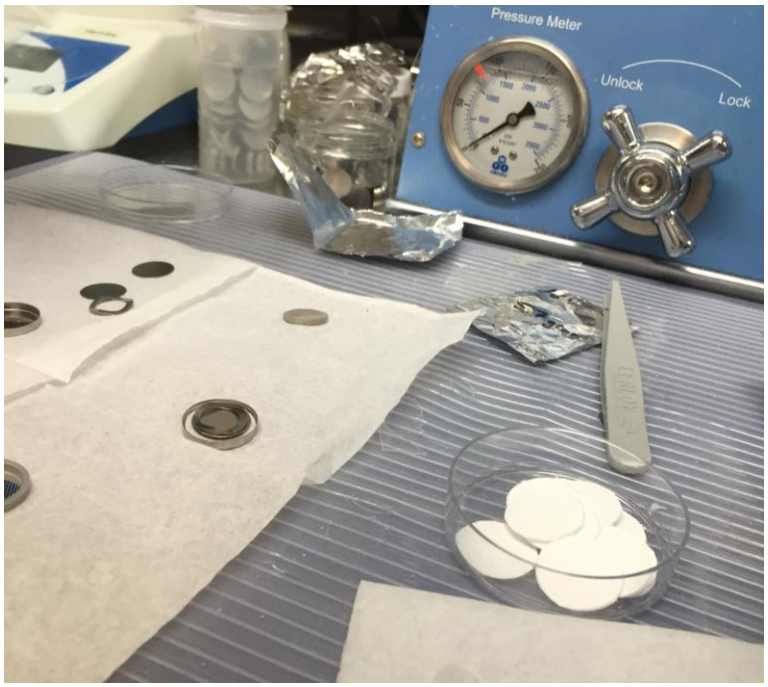

Figure 5: Coin Type Battery Preparation In A Glove Box

2.8 Characterization of $LiFePO_4$/PAN Nanofibers

A scanning electron microscope (SEM) was utilized to study the surface morphology of the $LiFePO_4$/PAN and $LiFePO_4$/C nanofibers. Elemental analysis was conducted with energy dispersive X-Ray spectroscopy (EDS), X-Ray photoelectron spectroscopy (XPS). For the $LiFePO_4$/C composite material, X-Ray Diffraction (XRD) and Raman was used to study the crystal structure. Once the battery cell was formed, electrochemical analysis was conducted.

CHAPTER III

RESULTS

3.1 Morphological Properties of $LiFePO_4$/PAN and $LiFePO_4$/C Composite Nanofibers

The surface morphology was studied by taking SEM images of pure PAN, $LiFePO_4$/PAN, and $LiFePO_4$/C composite nanofibers represented in figures 4.1, 4.2, and 4.3 respectively. Figure 6 shows a 10.7 wt.% PAN solution in DMF spun at 7000 – 9000 rpm with a fiber diameter ranging from 683 nm to 1.3 μm. This was used as a reference for comparison to the $LiFePO_4$ containing nanofibers to differentiate fiber diameter and fiber formation. Figures 7 and 8 show SEM images with a 1K magnification of LiFePO4/PAN nanofibers containing different wt.% of $LiFePO_4$ and all were spun at 7000 rpm for 2 min. As the $LiFePO_4$ wt.% increases this inversely affects the PAN concentration and causes the surface of the fiber to become coarse, non-homogeneous in fiber structure, and for bulky nodules to form within the fiber. This un-uniformity could be attributed to the spinning medium (PAN the polymer) decreasing as the $LiFePO_4$ concentration increases. It has been previously determined [7] that solutions consisting of PAN/DMF, as the PAN concentration falls below 12 wt.%, nodules or bead like structures along with thinner and brittle fibers are obtained.

The SEM images of the carbonized $LiFePO_4$/C composite nanofibers of the 2.4 Wt. % $LiFePO_4$ show well disbursement of the cathode material within and among the carbon

nanofiber. Conversely the 1.8 Wt. % $LiFePO_4$/C nanofibers don't show the cathode material well dispersed among the nanofiber.

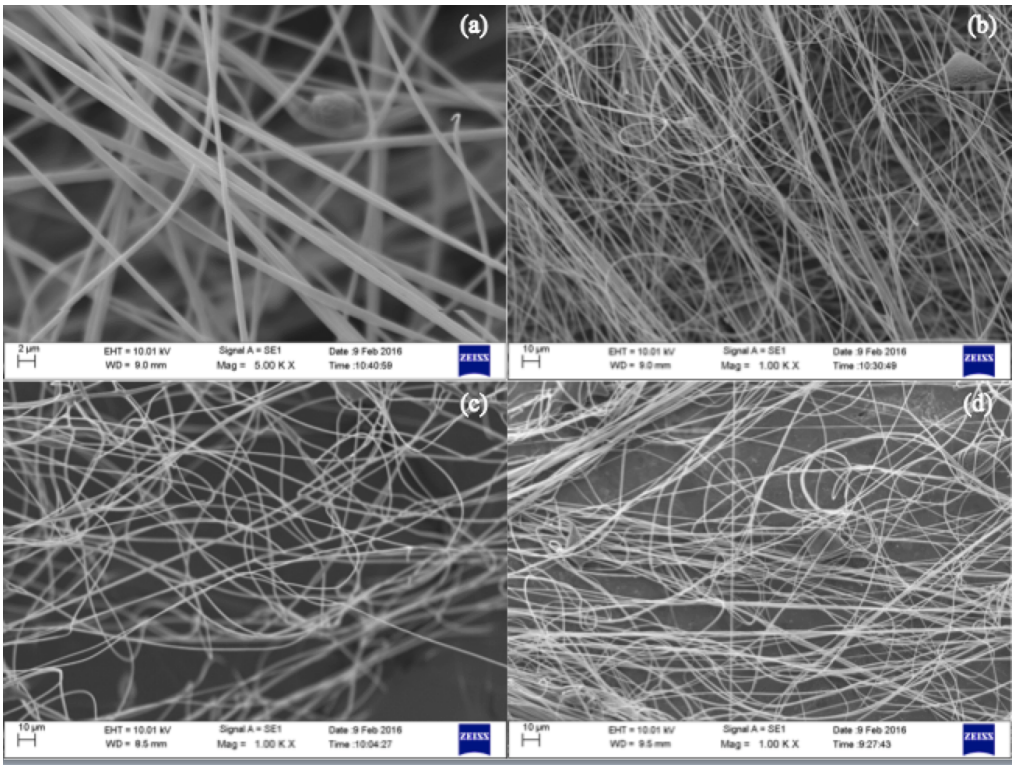

Figure 6. SEM images with 1K Magnification Forcespun® at a) 6000 rpm b) 7000 rpm c) 8000 and d) 9000 rpm.

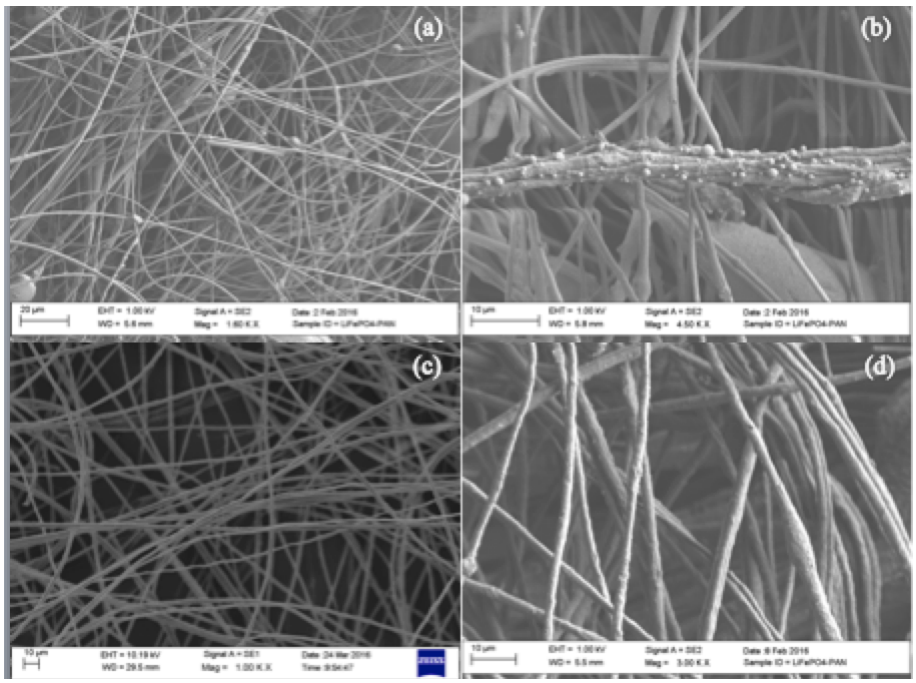

Figure 7. SEM Images of $LiFePO_4$/PAN Nanofibers Consisting of Different Wt.% of $LiFePO_4$ a) & b) 1.8 wt. % LiFePO4 c) 2 wt. % LiFePO4 and d) 2.4 wt. $LiFePO_4$

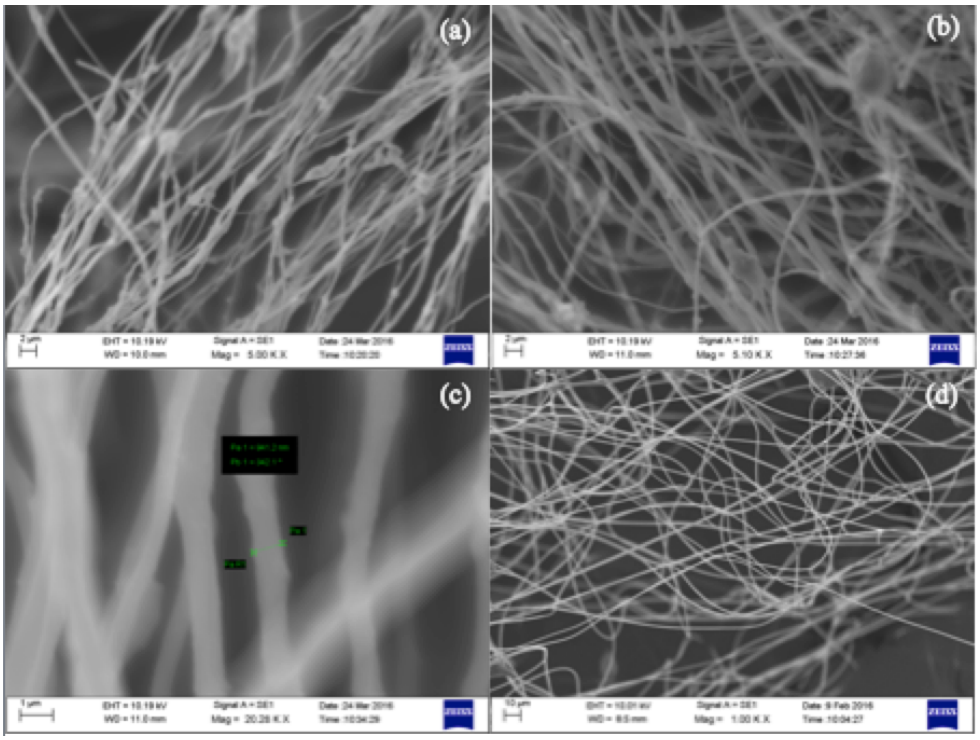

Figure 8. SEM Images of $LiFePO_4$/PAN Nanofibers Forcespun® at 7000 rpm Consisting of Different Wt.%'s of $LiFePO_4$ a) and b) 7 Wt. % LiFePO4 c) 8 Wt. % LiFePO4 d) SEM of 10.7 Wt.% PAN Solution for Reference

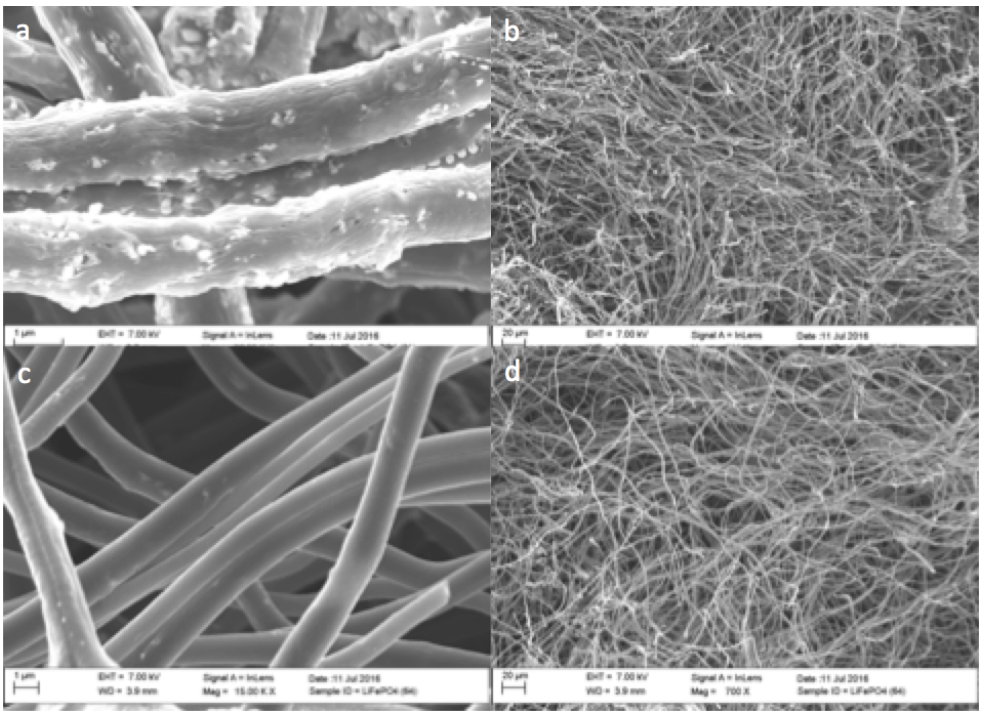

Figure 9. SEM Images of $LiFePO_4$/C Composite Nanofibers a) and b) 2.4 Wt.% $LiFePO_4$/C c) and d) 1.8 Wt.% $LiFePO_4$/C

Figure 10 shows the elemental analysis of nanofibers produced from a 2.4 wt.% $LiFePO_4$ solution. For this type of morphological study the EDS instrument is not sensitive enough to determine the Li content. Therefore only the contents of C, O, Fe, and P are observed.

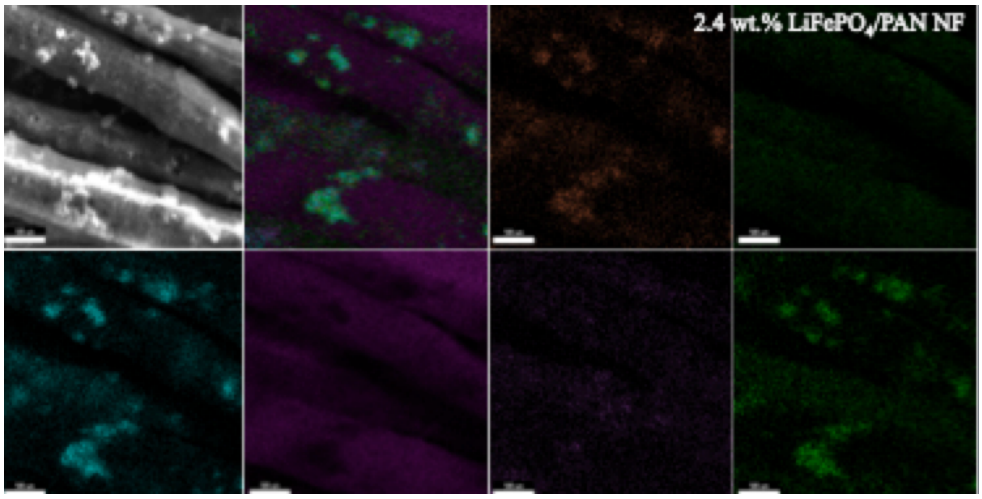

Figure 10. Elemental Analysis of $LiFePO_4$/PAN Nanofibers Consisting of 2.4 wt.% $LiFePO_4$

It can be deduced that $LiFePO_4$ nanocrystals are present on the surface of the nanofibers from the clusters of O, P, and Fe present.

3.2 Structural Analysis of $LiFePO_4$/C Composite Nanofibers

The crystal structure and determination of the phase composition of $LiFePO_4$/C composite nanofibers was studied via XRD analysis. Figure 11 shows the diffraction peaks of $LiFePO_4$/C composite nanofibers with different $LiFePO_4$ wt.%. There is a broad diffraction peak corresponding to 2θ of approximately 25° which according to the literature [1] is attributed to miller indices of 002. This confirms the presence of the disordered structure that corresponds to the carbon nanofiber matrix.

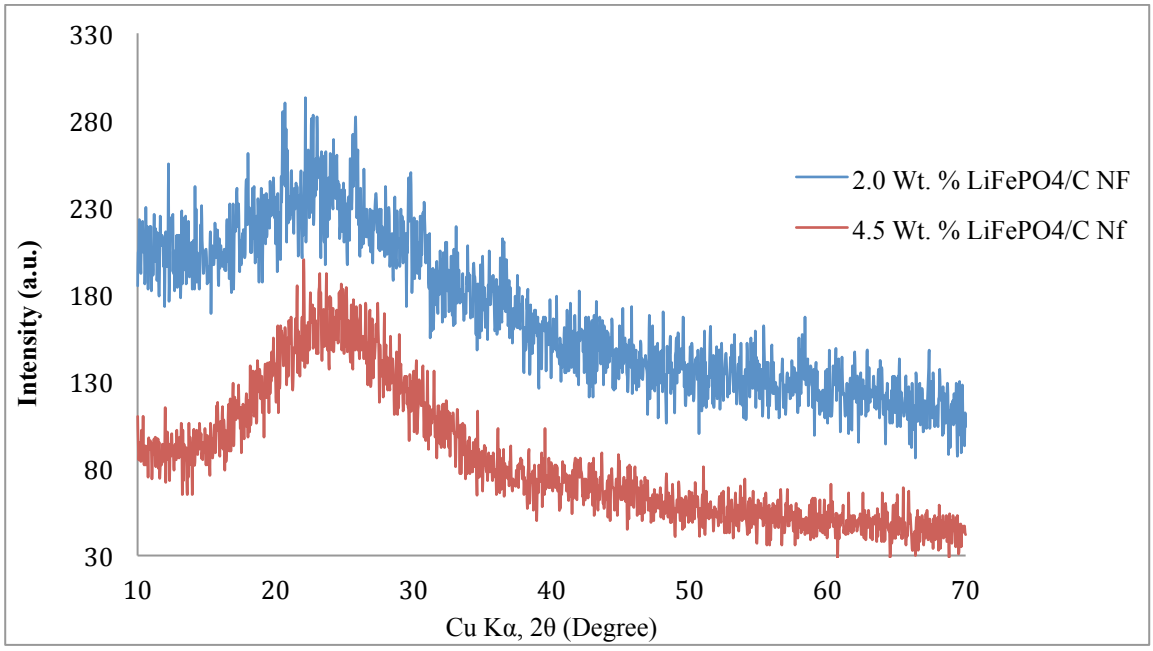

Figure 11. XRD Analysis of LiFePO4/C Composite Nanofibers with Different Wt. % of $LiFePO_4$

Although the carbon nanofiber structure is confirmed via XRD analysis, no peaks are present corresponding to the crystal structure of $LiFePO_4$. The lack of peaks could be attributed to not enough of $LiFePO_4$ present on the surface of the nanofiber or the overbearing intensity of the amorphous characteristic corresponding to the carbon nanofiber.

In order to determine not only the binding energy of the $LiFePO_4$ nanocrystal but also the presence of Li, Fe, P, and O- XPS analysis was conducted as shown in Figures 12– 15. Figure 12 shows an elemental survey scan of the surface of $LiFePO_4$/C nanofibers. Figure 13 shows the Li 1s region at its distinct peak at approximately 56 eV. Figure 14 shows the Fe 2p region and the corresponding major peak at 709 eV. Figure 15 shows the p 2p region and the corresponding peak at 134 eV. Due to the corresponding presence of Li, Fe, and P on the surface of the presumed $LiFePO_4$/C composite nanofiber, the existence of the $LiFePO_4$ nanocrystal is confirmed [1].

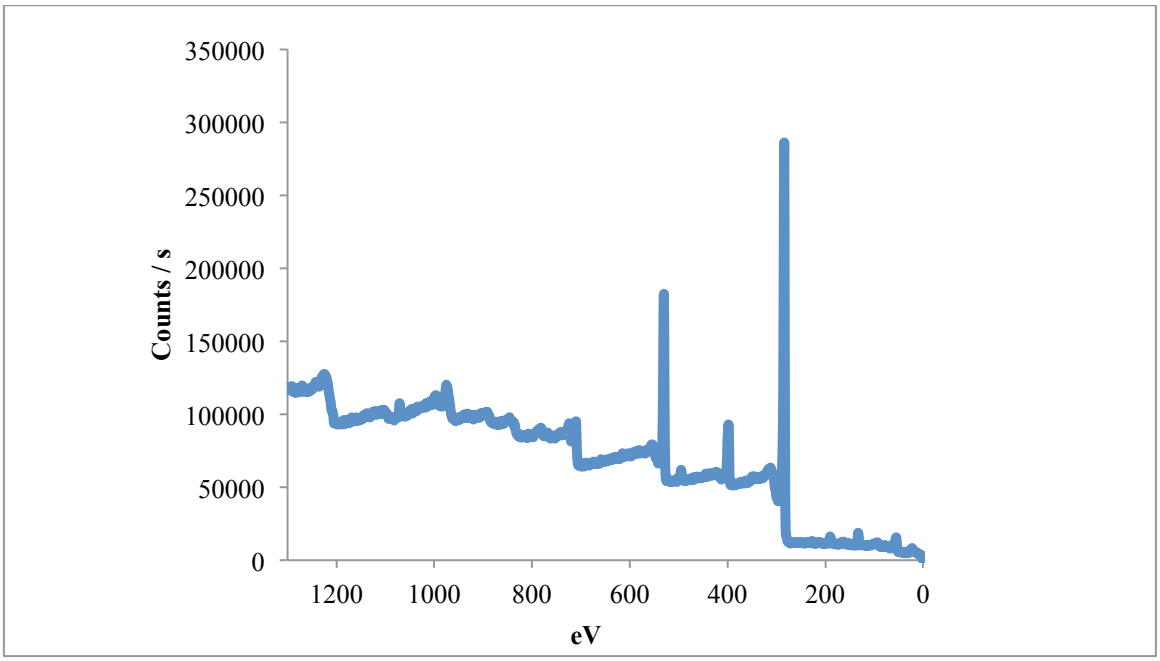

Figure 12. XPS Survey Scan of $LiFePO_4$/C Nanofibers Obtained from a 2.4 Wt.% Solution of LiFePO4

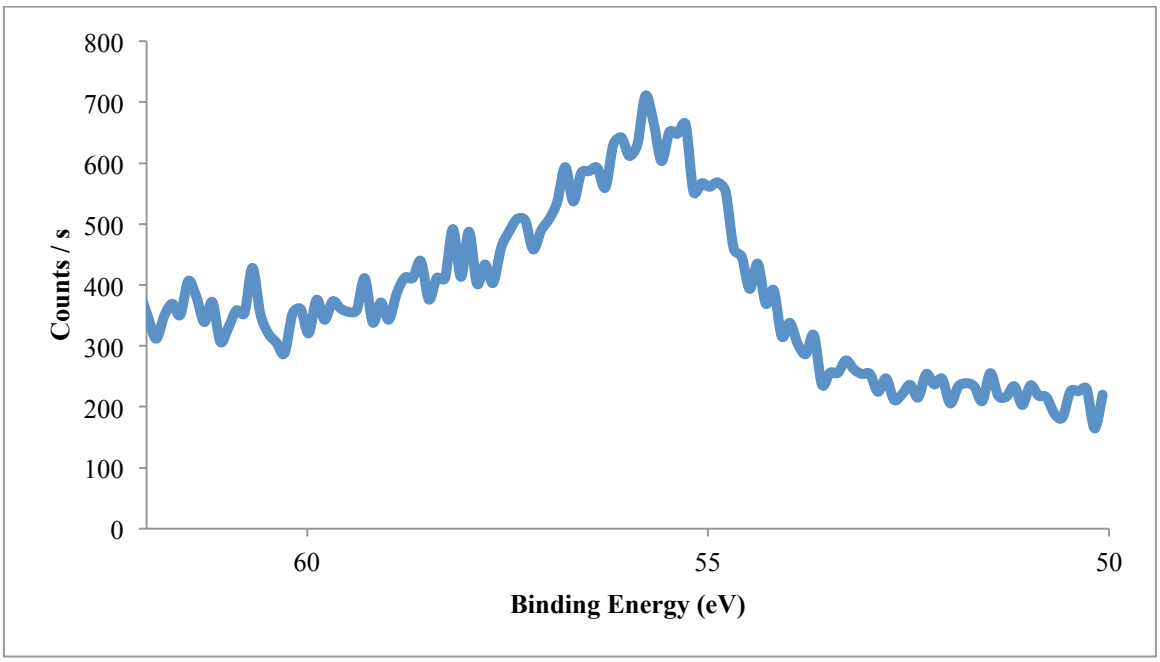

Figure 13. XPS Scan of Li 1s from $LiFePO_4$/C Nanofibers Obtained from a 2.4 Wt.% Solution of LiFePO4

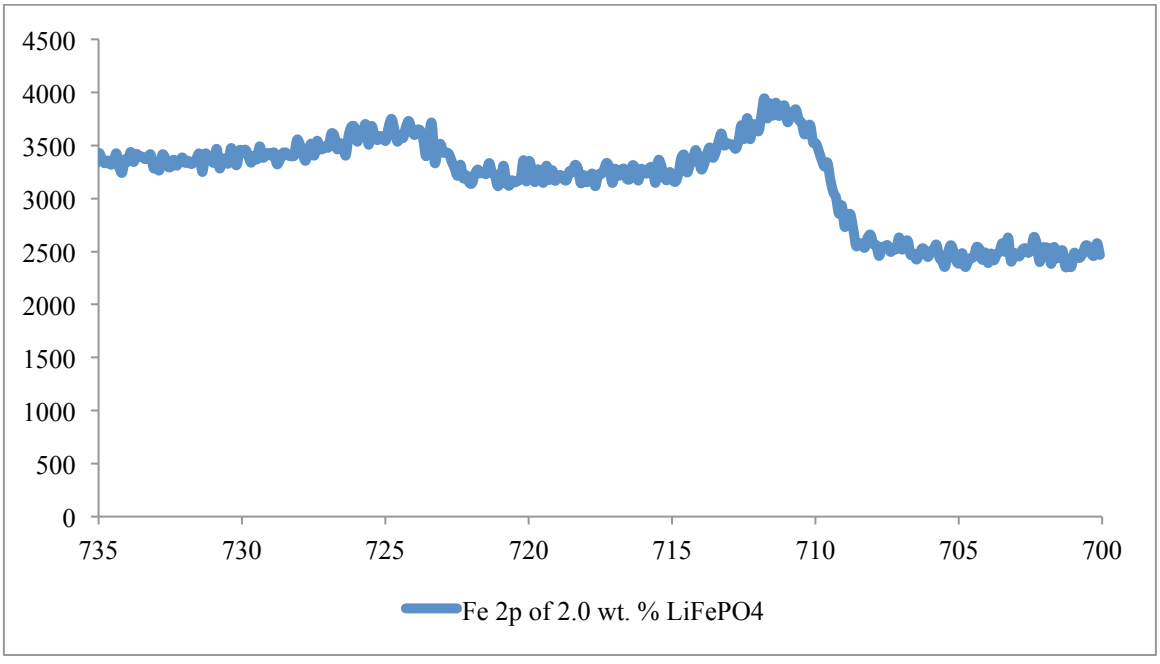

Figure 14. XPS Scan of Fe 2p from $LiFePO_4$/C Nanofibers Obtained from a 2.4 Wt.% Solution of LiFePO4

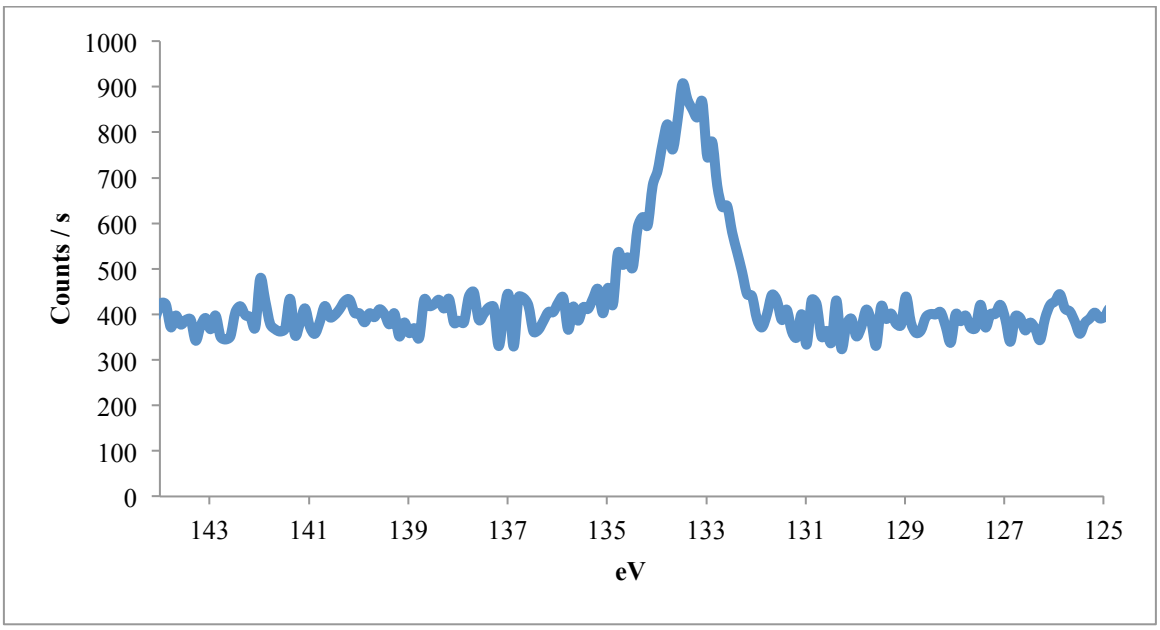

Figure 15. XPS Scan of P 2p from $LiFePO_4$/C Nanofibers Obtained from a 2.4 Wt.% Solution of $LiFePO_4$

The Raman spectrum is a compilation of all four samples producing fibers. Each sample shows a slight D-band that is attributed to a disorder-induced phonon mode within the range of 1200 cm^{-1} – 1350 cm^{-1} [6]. Each sample also shows a strong G-band, which pertains to a prominent graphite band within the ranges of 1600 cm^{-1} – 1700 cm^{-1}. Lastly, a third band that does not correlate to published data occurs in all four samples within the range of 2200 cm^{-1} – 2400 cm^{-1}. This is attributed to a 2D-band corresponding to the possibility of the carbon nanofiber containing multiple layers of graphite [8].

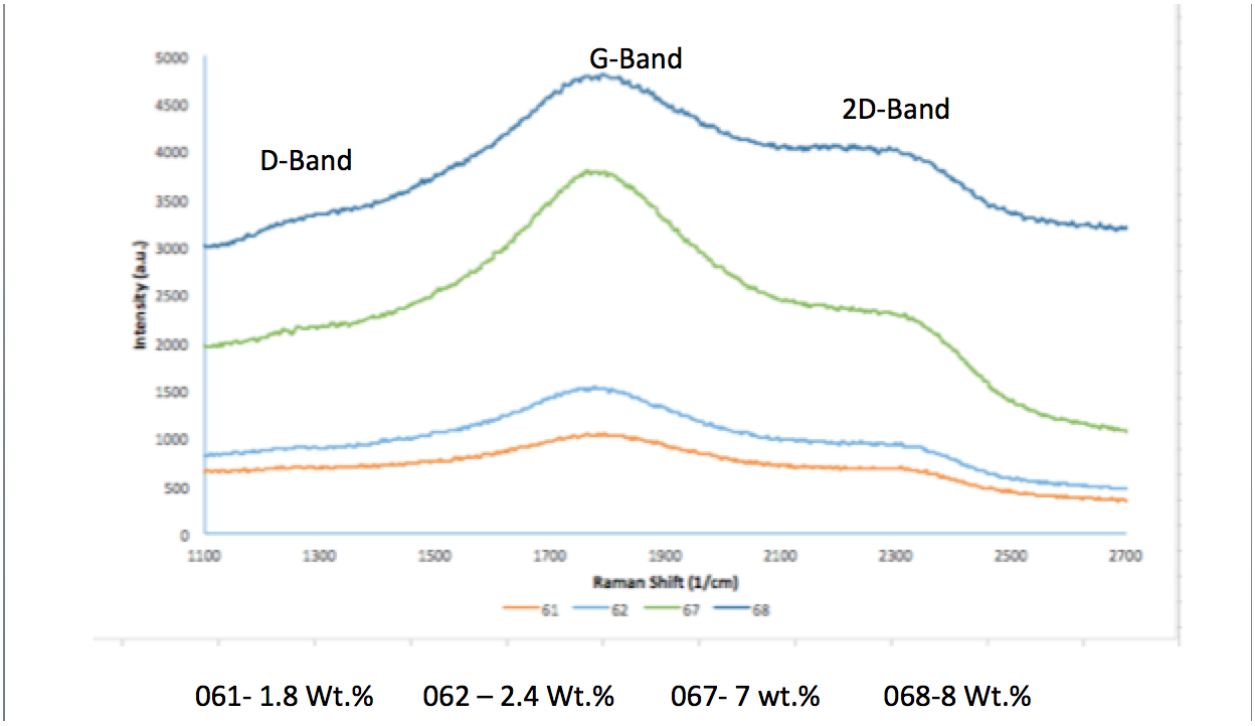

Figure 16. Raman Spectra of carbonized Submicron-Fibers

CHAPTER IV

CONCLUSION

SEM concluded the nanoparticles were evenly distributed amongst the submicron-fiber for the carbonized 2.4 Wt.% $LiFePO_4$/C and the diameter ranged from 0.7 μ – 1 μ. EDS proved the clumps of nanocrystals correspond to the Fe, P, and O contained within the cathode material on the $LiFePO_4$/PAN nanofibers. XPS of the carbonized LiFePO4/C NF concluded the presence of Li, which is not picked up in most characterization techniques. Raman concluded the presence of G-band and a slight D-band analogous to published data and also a third band that does not correspond to published data [1]; the 2D band. XRD confirms the diffraction peak at around 25 ^{o}C which signifies the disordered structure of the CN matrix.

REFERENCES

1. Liwen Ji, Ozan Toprakci, Mataz Alcoutlabi, Yingfang Yao, Ying Li, Shu Zhang, Bingkun Guo, Zhan Lin, and Xiangwu Zhang (2012). α-Fe_2O_3 nanoparticle-loaded carbon nanofibers as stable and high-capacity anodes for rechargeable Lithium-ion batteries. *Applied Materials and Interfaces*, 4, 2672-2679.

2. Liwen Ji, Zhan Lin, Mataz Alcoutlabi and Xiangwu Zhang (2011). Recent developments in nanostructured anode materials for rechargeable lithium-ion batteries. *Energy and Environmental Science*, 4, 2682-2699.

3. Dan Li and Younam Xia (2004). Electrospinning of Nanofibers: Reinventing the wheel? *Advanced Materials*, 16(14) 1151- 1170.

4. Victor A. Agubra, Luis Zuniga, David Flores, Jahaziel Villareal, Mataz Alcoutlabi (2016). Composite nanofibers as advanced materials for Li-ion, Li-O_2, and Li-S batteries. *Electrochimica Acta* 192, 529-550.

5. Kamal Sarkar, Carlos Gomez, Steve Zambrano, Michael Ramirez, Eugenio de Hoyos, Horacio Vasquez, Karen Lozano (2010). Electrospinning to Forcespinning^{TM}. *Materials Today*, 13(11) 12-14.

6. Ozan Toprakci, Hatice A.K. Toprakci, Liwen Ji, Guanjie Xu, Zhan Lin, and Xiangwu Zhang (2012). Carbon nanotube-loaded electrospun $LiFePO_4$/Carbon composite nanofibers as stable and binder-free cathodes for rechargeable lithium-ion batteries. *Applied Materials and Interfaces,* 4, 1273-1280.

7. Baicheng Weng, Fenghua Xu, Karen Lozano (2014). Mass production of carbon nanotube-reinforced polyacrylonitrile fine composite fibers. *Journal of Applied Polymer Science* 131(11) app. 40302.

8. Andrea C. Ferrari (2007). Raman spectroscopy of graphene and graphite: Disorder, electron-phonon coupling, doping and nonadiabatic effects. *Solid State Communications* 143, 47-57.

9. Ozan Toprakci, Liwen Ji, Zhan Lin, Hatice A.K. Toprakci, Xiangwu Zhang (2011). Fabrication and electrochemical characteristics of electrospun $LiFePO_4$/carbon composite fibers for lithium-ion batteries. *Journal of Power Sources* 196, 7692-7699.

10. Changhuan Zhang, Lan Yao, Yiping Qiu (2016). Synthesis and characterization of $LiFePO_4$-carbon nanofiber-carbon nanotube composites prepared by electrospinning and thermal t reatment as a cathode material for lithium-ion batteries. *Journal of Applied Polymer Science* 133, app 43001.

11. Mataz Alcoutlabi, Hun Lee, Jill V. Watson, Ziangwu Zhang (2013). Preparation and properties of nanofiber-coated composite membranes as battery separators via electrospinning. *Journal of Material Science* 48, 2690-2700.

12. Ozan Toprakci, Hatice A.K. Toprakci, Liwen Ji, Zhan Lin, Renpeng Gu, and Xiangwu Zhang (2012). $LiFePO_4$ nanoparticles encapsulated in graphene-containing carbon nanofibers for use as energy storage materials. *Journal of Renewable and Sustainable Energy* 4, app 012121.

13. Changhuan Zhang, Yinzheng Liang, Lab Yao, Yiping Qiu (2015). Effect of thermal treatment on the properties of electrospun $LiFePO_4$-carbon nanofiber composite cathode materials for lithium-ion batteries. *Journal of Alloys and Compounds*, 627, 91-100.

14. Zhipeng Ma, Guangjie Shao, Yuqian Fan, Guiling Wang, Jianjun Song, and Tingting Liu (2014). *Applied Materials and Interfaces*, 6, 9236-9244.

BIOGRAPHICAL SKETCH

Ashlee L. Lopez was born in Harlingen, TX on February 16. 1991 and grew up in Weslaco, TX. She graduated from South Texas High School for the Health Professions in 2009 and proceeded to obtain her bachelor's degree in chemistry from The University of Texas Pan-American in 2013 in Edinburg, TX. In January of 2014 she got accepted into the graduate program at The University of Texas Rio Grande Valley to obtain a master's degree in chemistry. She then began research with Dr. T. Atesin pertaining to carbonized submicron particles for cathode applications. Lastly she obtained her MS in Chemistry in 2017. She currently resides in Austin, TX with her husband, Ramon Ocanas III and their dachshund Audrey. For future correspondence opportunities email: ashlee.lizette@gmail.com.